Process Safety and Environmental Protection 144 (2020) 330–336

Contents lists available at ScienceDirect

Process Safety and Environmental Protection

journal homepage: www.elsevier.com/locate/psep

Multiphase CFD modeling and laboratory testing of a Vortecone for mining and industrial dust scrubbing applications

Ashish Ranjan Kumar*, Steven Schafrik

Department of Mining Engineering, University of Kentucky, Lexington, KY, United States

ARTICLE INFO

Article history:
Received 28 March 2020
Received in revised form 10 May 2020
Accepted 29 July 2020
Available online 1 August 2020

Keywords:
Dust scrubber
Optical particle counting
Computational fluid dynamics modeling
Cleaning efficiency
Multi-phase flows
Mining engineering

ABSTRACT

Dust exposure-related occupation diseases are irreversible and have led to debilitating outcomes in personnel. Particles like coal dust generated in mines and accumulated above a critical concentration are explosive. Fibrous type multi-layered filters are the primary dust particle capturing element in flooded-bed dust scrubbers. However, these filters get clogged due to prolonged dust accumulation. This paper investigates the interaction of dust, water, and airflow in CFD in a non-clogging Vortecone filter. The Vortecone accelerates the particle-laden fluid, forces it into rapid swirling fluid motion, and pushes particles to separate and capture them. Filter capture performance in several air and water quantities regimes with aerosol particles exceeding 2.0 μm from a coal-dust laden airstream is described here. Detailed computational fluid dynamics models mimicking steady-state flow regime and transient-state air-water interface motion are presented. Particle tracking and their capture on water film using volume of fraction approach to determine the cleaning efficiency for different particle sizes is presented. Experimental cleaning efficiency results obtained from iso-kinetic sampling and optical particle counting agree with the computer models. Laboratory tests run on the Vortecone showed coal-dust cleaning efficiency exceeding 75% for particles 2.8 μm in size and 90% for 4.7 μm for all airflows.

1. Introduction

Dust generation is associated with all unit operations in mining and many other industrial setups (Petavratzi et al., 2005). This brings allied health and safety nuisance with it. Prolonged exposure to dust has been shown to contribute to the onset of many debilitating diseases. Occupational diseases like asbestosis and coal workers' pneumoconiosis have led to the death of thousands of workers. Industries, therefore, adopt a variety of remedial measures to lower the exposure of personnel. However, coal workers' pneumoconiosis (CWP) associated with underground mining operations has seen a recent upsurge, especially in the Appalachia region in the eastern United States (Arnold, 2016; Laney and Weissman, 2014). Coal dust also forms an explosive mixture with air when present in critical concentrations. Research has also shown that explosion depends on numerous factors including space, time, volatile ratios, and ignition sources (Zheng et al., 2009). Methane explosion immediately followed by a coal dust explosion in Upper Big Branch led to 29 fatalities (MSHA, 2014a). Thirteen miners lost their lives in two separate explosions in Jim Walter Resources mine (MSHA, 2002).

Legislation including the Federal Coal Mine Health and Safety Acts of 1969 and 1977 established specific rules to ensure the safety of workers in the United States (MSHA, 1969; MSHA, 1977). The 'Final Rule' was enacted in 2014 after a series of fatal events and called for additional measures to reduce dust levels to lower concentrations underground in general working areas and the return airways (MSHA, 2014b). Dilution of generated dust to harmless levels by underground mine ventilation airflow is the mainstay of dust combating systems. Water sprays are also used to redirect the dust-laden air away from the personnel to lower their exposure. Sprays have also been shown to capture airborne dust (Pollock and Organiscak, 2007). Fine particles are especially difficult to remove from the airstream and suitable scrubbers are required to have numerous engineering controls (Calvert, 1974). Wet scrubbers are efficient in capturing small particles up to 5.0 μm (Eckert and Stringle, 1974). The mining industry has seen a lot of research towards the development of active scrubbing systems, including ventilated drums, cowls, and numerous machine mounted scrubbers.

Flooded-bed dust scrubbers are installed on continuous mining machines to capture the dust generated at the blind headings (Campbell et al., 1983; Colinet et al., 2013). These scrubbers have

* Corresponding author at: 504 Rose Street, 109, Mining and Minerals Resources Building, Lexington, KY, 40506, United States.
E-mail addresses: ashish.kumar@uky.edu (A.R. Kumar), steve.schafrik@uky.edu (S. Schafrik).

https://doi.org/10.1016/j.psep.2020.07.046
0957-5820/

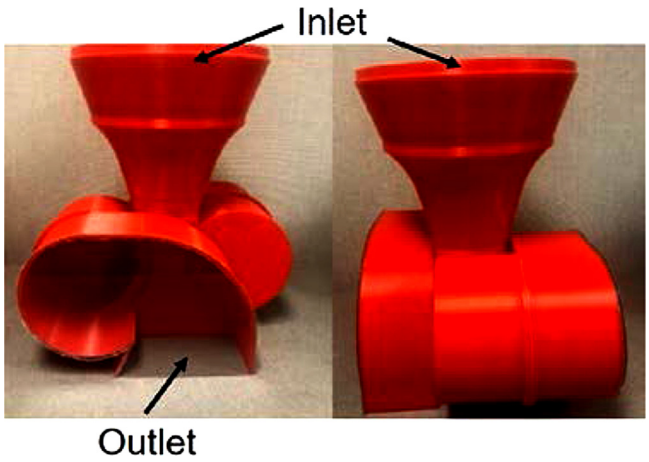

Fig. 1. A 3D printed demonstration model of the Vortecone invented at the Institute for Research in Technology Development, University of Kentucky.

water flooded fibrous filter element to capture airborne dust and a demister to remove water droplets from the air. A modified version of these scrubbers was proposed for a specific longwall shearer by the mining engineering department at the University of Kentucky (Wedding et al., 2015). However, the multi-layered fibrous filters used in these scrubbers are prone to clogging (Thomas et al., 2001). This results in a progressively higher resistance and an elevated pressure drop to airflow due to dust entrapment on the filters (Calle et al., 2001; Agranovski and Shapiro, 2001; Kanaoka and Hiragi, 1990). This leads to a lowered capture of dust-laden air and hence a drop in the overall efficiency of the scrubbing system. These filters also need to be cleaned frequently which leads to low productivity of the mining machine since they are not allowed to operate without the dust scrubber running. Impactors were designed in the early 1970s to classify dust particles based on their size and momentum. Larger particles are captured on earlier stages since they cannot negotiate sharp turns easily and impact one of the many filter surfaces (Marple and Willeke, 1967; Newton et al., 1977). This research investigates the operations of a wet Vortecone scrubber with its major axis oriented in the vertically upright orientation. The research specifically examines the performance of the filter with different particle sizes.

A Vortecone similar to one shown in Fig. 1 was invented at the Institute for Research in Technology Development, the University of Kentucky to capture over-sprayed paint particles from vehicle painting lines (Salazar et al., 2002; Salazar et al., 2000). Particle-laden air is brought into the Vortecone and accelerated to much higher velocities assisted by a continuously decreasing area of the cross-section. The air is discharged into the vortex chamber where it undergoes a rapid circulatory motion separating the particles like a cyclone scrubber (Krames and Buttner, 1994). Water is injected into the Vortecone using a full-cone spray. Water from the spray turns into rapidly swirling films on the surface. The Vortecone captures particles from the airstream by differentially altering their trajectories. The heavier dust particles are removed from the air stream and sent towards the outer periphery where they are trapped by the water film close to the surface (Dahneke, 1971). With no fibrous filter or moving parts, the Vortecone is a maintenance-free equipment. A reduced scale model of the Vortecone was used for numerical modeling and laboratory experiments. Computational fluid dynamics (CFD) models were first generated to examine the flow pattern, and film and particle transportation before running complex and expensive laboratory experiments.

Authors present 3D CFD models representing the steady-state flow regime in the Vortecone. Transient state free-surface and Lagrangian particle tracking techniques were used to predict the trend of cleaning efficiency and are discussed in detail. Particles were modeled to be trapped on the air-water interface predominantly close to the vortex chamber surface. A test set-up was constructed to test the performance parameters of the Vortecone and to validate the computer models. Two identical TSI optical particle sizers (OPS 3330) were installed upstream and downstream of the Vortecone to count and size the coal dust particles. Keystone mineral black 325 A sample was used as the feed dust to determine the cleaning efficiency. Results from laboratory testing are presented later and are compared to the computer models.

Table 1
Mesh and flow parameters for grid independence studies.

Parameters	Mesh 1	Mesh 2	Mesh 3
Number of elements, N	488,784	1,109,136	2,552,806
Average cell dimension (mm)	3.04	2.31	1.75
Magnitude of velocity, ϕ_1	32.44	32.40	32.12
Magnitude of velocity, ϕ_2	63.58	63.14	63.35
Magnitude of velocity, ϕ_3	63.02	63.74	62.36

2. Computational fluid dynamics (CFD) modeling

The computational fluid dynamics modeling technique was used to numerically mimic the multi-phase particle-laden fluid flow for this research. A computer modeling approach was adopted because flow inside the Vortecone is very sensitive to the geometry and any instrumentation would have influenced the flow profile and parameters. The software scFLOW, version 14 was used for its excellent ability to generate high-quality unstructured meshes in the complex geometry of the Vortecone. To generate the CFD models, the 3D-structure of the Vortecone was first drawn and imported into scFLOW. A vertical plane of symmetry passing through the inlet was used to bifurcate the flow-volume to save on computing resources. Flow volumes and surfaces were assigned unique names and octree composed of a cluster of cubical cells was produced. The octree cell size was controlled with smaller cells placed close to the impermeable surfaces and in regions of large pressure gradients. Five prism layers were inserted on the impermeable surface to model the boundary layer phenomenon. Boundary conditions included flux with appropriate turbulence parameters and wall functions. This was followed by transient state free-surface models and particle tracking.

2.1. Steady-state models

Steady-state flow fields were established first to determine the operating points. Boundary conditions included flux at the inlet, static pressure at the outlet, and suitable wall functions on all other surfaces for the steady-state flow regime. The realizable κ-ε turbulence model was used for its good abilities to model circulating flows and large pressure gradients. The simulations were run until the set threshold residual of convergence of 0.0001 in all velocity components and pressure were met. Mesh independence studies were then carried out to ascertain the numerical robustness of the grid. Errors in velocity magnitude at three points inside the flow domain were investigated for this. Table 1 shows the grid parameters and velocity values at three grid points inside the Vortecone. These points were chosen close to the inlet guide, close to the sharp curve at the bottom, and the outer periphery of the vortex chamber. Richardson's method of calculating the errors was used (Celik et al., 2008). Excel solver was used for these computations and results are compiled in Table 2. The average relative error, the extrapolated error, and the average fine grid convergence index were computed to be 0.89%, 0.83%, and 1.03 respectively which indicates strong mesh independence.

Table 2
Error and grid convergence index calculations.

Parameters	Symbol	Mesh 1	Mesh 2	Mesh 3
Approximate relative errors (%)	e_a^{21}	0.87	0.33	2.21
	e_a^{32}	0.12	0.70	1.13
Extrapolated values of velocity (m/s)	$\phi^{ext}{}_{21}$	32.07	63.53	60.78
	$\phi^{ext}{}_{32}$	32.39	62.74	64.58
Extrapolated errors in velocity (%)	e_{ext}^{21}	0.15	0.29	2.60
	e_{ext}^{32}	0.02	0.63	1.31
Fine grid convergence index	$GCI_{fine}{}^{21}$	0.19	0.36	3.17
	$GCI_{fine}{}^{32}$	0.03	0.78	1.66

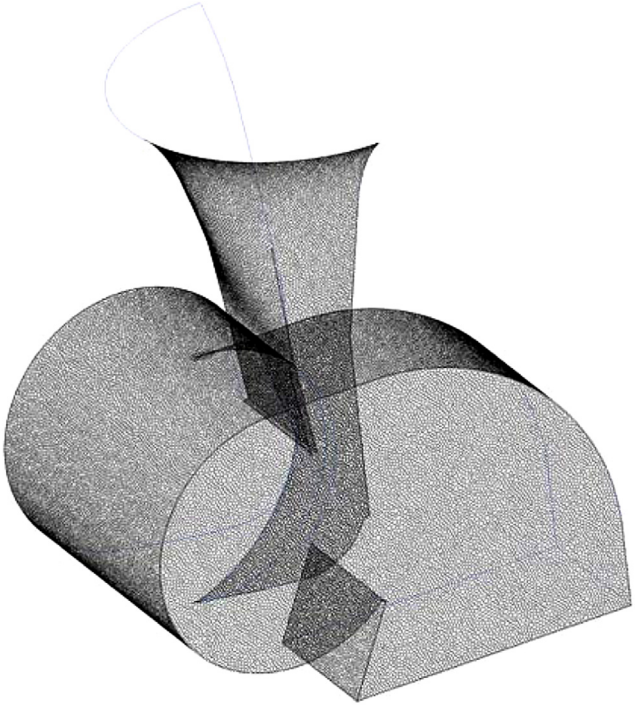

Fig. 2. Polyhedral mesh on the surface.

Once strong grid independence was established, the second mesh as shown in Fig. 2 with about 1.10 million grid elements was used to generate steady-state flow fields with different airflows resulting in a system curve. Scalar integration of normalized wall distances ($y+$) on the impermeable surfaces was carried out as a final check to examine mesh quality. An average $y+$ value of 9.28 was obtained, which indicates that the mesh is fine enough to resolve the flows close to the walls. Fig. 3 shows contours of velocity magnitude on parallel planes through the Vortecone for an airflow of 0.38 m^3/s through the system. Velocity vectors indicate fast-moving circulating air close to the periphery. Air is observed to accelerate to high speeds compared to the incident airflow speed at the Vortecone inlet.

2.2. Transient state models

Transient-state models were generated to mimic the formation and dynamics of thin films for 1.0 s after the fluids were released in the Vortecone. Owing to the computationally expensive nature of the multi-phase simulations, one fixed water flow of 15.1 l/min for two different airflows of 0.28 m^3/s and 0.38 m^3/s was modeled. Results from the converged steady-state models were adopted in these models as steady-state field input and to save on computing resources. Due to the fineness of the mesh required to capture the interfaces precisely and nature of the flow, a small time-step of

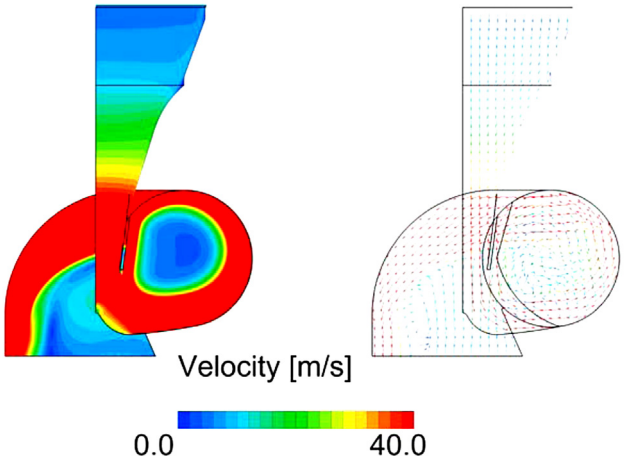

Fig. 3. Contours of velocity magnitude and velocity vectors for an airflow of 0.38 m^3/s.

the order of 50.0 μs was used to keep the average Courant number under 1.0 for the entire duration of transient state simulations including the free-surface models and particle-tracking.

The physical dimensions and operating parameters of the spray (6.4 mm opening diameter, 110° external spray angle) were adopted from the manufacturer catalog to generate the films. The volume of fraction (VOF) approach was followed to trace the air-water interface in the Vortecone (Hirt and Nicholas, 1981). This is a powerful mathematical technique adopted to model moving fronts in a flow domain. Dry air was assigned a VOF value of 0.00 while pure water was imparted the value of 1.00. All cells with fractional VOFs consisted of the air-water interface. Discrete water droplets of size 50.0 μm and with the properties of liquid water at 20 °C were assumed to be delivered by the spray. The discrete water particles were programmed to undergo a perfectly inelastic collision with the impermeable surfaces of the Vortecone. The particles were stored as an equivalent VOF on the surface and allowed to coalesce and grow. This led to the formation of a continuous iso-surface of VOF resulted in depicting the air-water interface and was used for particle capture later. This also led to the elimination of numerical diffusion problem which is encountered in modeling multi-phase flows. Iso-surface of VOF of 0.01 is shown in Fig. 4. A higher VOF to represent the film would require very fine mesh and hence massive computing resources to represent the same air-water interface. A chaotic unpredictable trend of mass flow rates at the outlet as shown in Fig. 5 for the airflows indicates an unsteady and highly turbulent flow regime in the Vortecone. Negative numbers indicate that the fluids move out of the computational domain from the outlet surface.

Lagrangian method of particle tracking was used to model the transportation of uncharged solid spherical dust particles ranging in size from 2.0 to 14.0 microns. Cunningham's slip correction factor was applied to all those particles to account for precise drag computations (Cunningham, 1910). Stream of aerosol particles was generated randomly at the inlet surface and injected normal to it into the Vortecone. The particles were tracked in small time-steps as they were transported inside. The particles were programmed to get destroyed at the outlet of the Vortecone. To ensure that the particles are not captured by the dry impermeable surface of the Vortecone, the particles were assumed to undergo an elastic collision with the walls with a coefficient of restitution of 0.95 (Tsai et al., 1990). To mimic the capture of dust particles on the rapidly moving surface of the water, a formatted user-defined script was written to extract information on the position and velocity components of the particles. The script sets the particles' velocity to

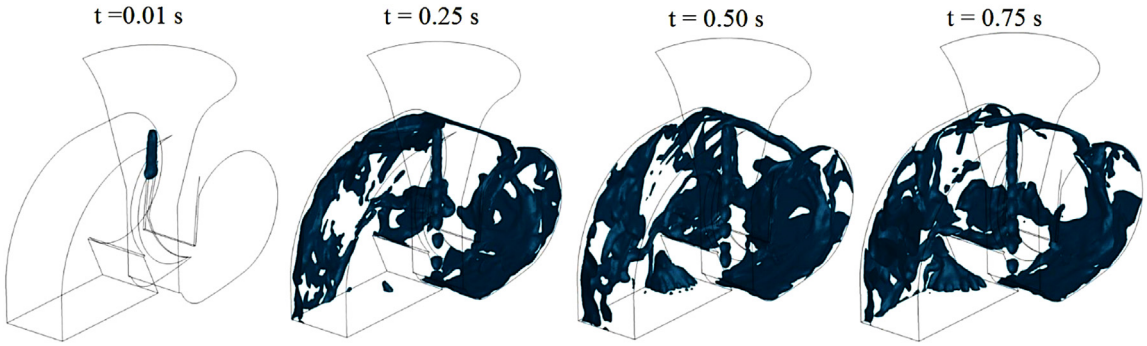

Fig. 4. Iso-surfaces of the volume of fraction of 0.01 in the Vortecone.

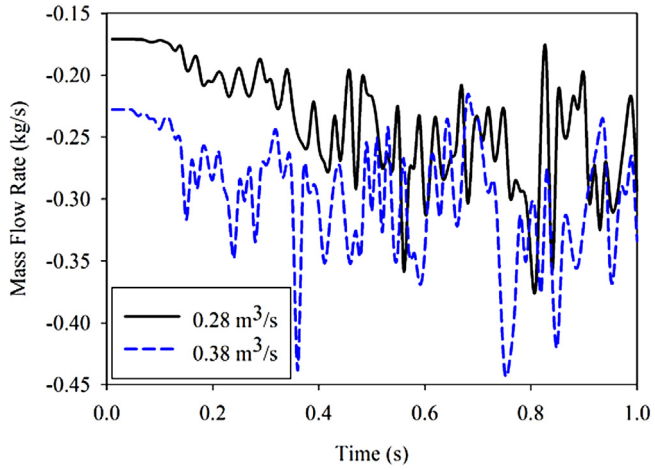

Fig. 5. Mass flow rates at the outlet for the two airflows and a water inflow of 7.57 l/min.

be 0.00 m/s and their diameter to be 0.0 μm whenever they travel into a mesh cell with a pre-assigned VOF at any given instant. This numerically represents trapping of the particles by the air-water interface since the affected particles are rendered immobile and do not report to the Vortecone outlet. The particles were counted and classified based on their diameter. The difference in particle count at the outlet between the inlet and the outlet of the Vortecone yields the numerical cleaning efficiencies for that diameter. A parametric study of the VOF was carried out and trends of cleaning efficiency generated for the two airflows. The plots were then compared with the laboratory experiments and are shown together later in this paper.

3. Laboratory testing of the vortecone

Laboratory experiments were designed and set-up to investigate the cleaning efficiency of the Vortecone. A centrifugal fan controlled by a variable frequency drive (VFD) was used to force air through the Vortecone to determine its cleaning efficiency. Ductwork measuring 2.40 m in length and with cross-section dimensions of 0.48 m X 0.30 m attached to the fan. Vane rail arrangements were incorporated to maintain the streamlines of flow and to lower the pressure drop due to shock losses at the bends. Vortecone was installed with its primary axis in a vertical direction as shown in Fig. 6. The figure shows the lobes of the vortex chamber and a means to inject water using collars or simply by mounting a spray pointing into the Vortecone. A water spray described in the modeling section above was installed facing the vortex chamber and held stationary. The fluid inlet is on the top while the outlet is at the bottom of the Vortecone in all the figures. Total and static pressures were recorded at the Dwyer measurement station with honeycomb-like flow straighteners built into the ductwork.

3.1. Test procedure to determine the flow-pressure drop curve

The system curve for the Vortecone system was established first. A frequency of 15.0 Hz was set on the VFD and total and static pressure measured. Velocity pressure being the difference of total and static pressures yielded the average airflow speed through the system at the known pressure. The frequency was stepped up in steps of 5.0 Hz until 40.0 Hz and the process repeated three times to get a good representative average. The system (flow-pressure) curve of the form of a quadratic dependence of pressure on volumetric flow rates as shown in Fig. 7. The steady-state simulation results obtained from CFD models are also shown alongside and agree well with the laboratory experiments.

3.2. Test procedure for cleaning efficiency

Experiments were set-up and run to investigate the cleaning efficiency of the Vortecone. A full-cone water spray (1/2 –HH – 40 - WSQ) was installed to introduce water into the Vortecone. The term HH-WSQ indicates that the spray orifice is of male type and its connection size varies between 3.175–25.4 mm (1/8 – 1 in.). The spray is constructed of brass, mild steel, stainless steel, or poly-vinyl chloride. The spray used in the experiments has a discharge diameter of 6.4 mm and an outer spray angle of 110°. A digital flow meter with a control knob was connected in series for precise injection of water. Keystone Mineral Black 325 A was used for cleaning efficiency testing owing to the known particle size distribution. A 3D printed auger-feeder connected to an Arduino controlled stepper motor was used for precise dust injection. A code was written and compiled that controlled the rotational parameters of the feeder including angular speed and displacement. This controlled the rate of dust fed upstream of the filter. This was critical because a higher injection rate of dust particles would have resulted in co-incidence errors and particles would have been sampled incorrectly. The dust particles were injected pneumatically into the highly pressurized ductwork using the laboratory supply of compressed air to overcome the pressure developed by the fan.

TSI OPS 3330 with a fixed pump flow rate of 1.0 l/min was used to sample the airflow to count and size the aerosol particles optically. For this, customized nozzles sized to meet this airflow requirement through the OPS were designed and 3D printed. This was done to sample the airflow iso-kinetically for collecting a rep-

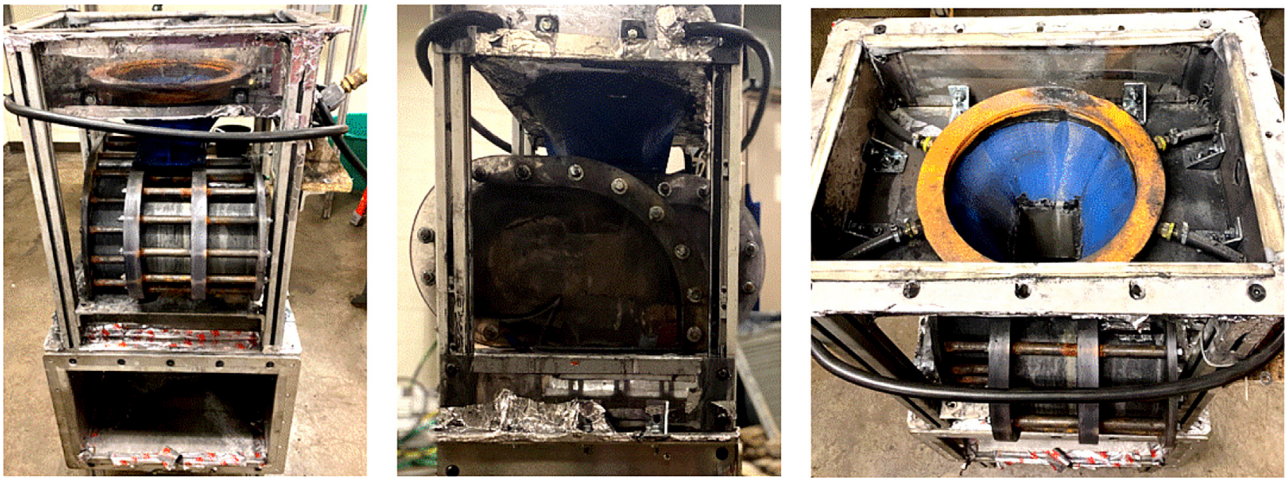

Fig. 6. The Vortecone used for laboratory experiments.

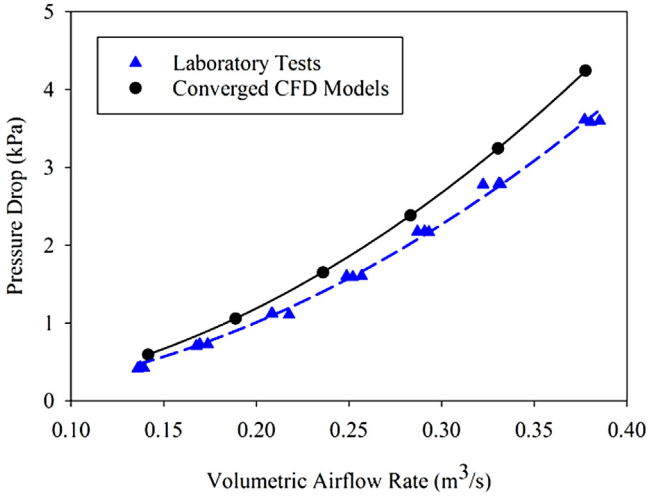

Fig. 7. Flow-pressure curve for the Vortecone.

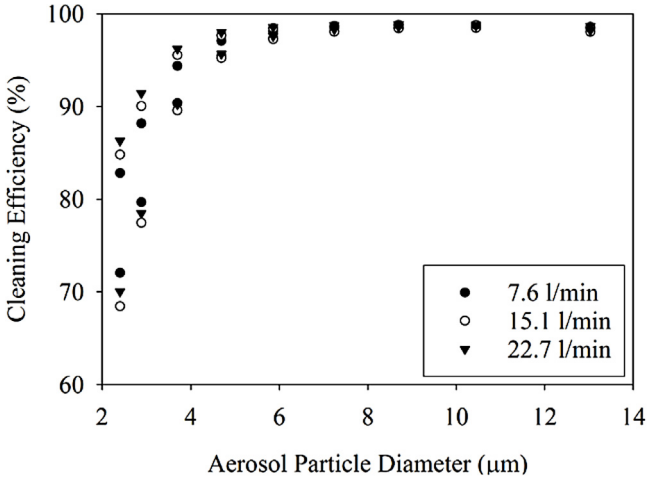

Fig. 8. Cleaning efficiency plot obtained at the airflow of 0.28 m^3/s.

resentative sample of particle-laden airflow and to avoid under or over-sampling of flows (Wilcox, 1956). A dead-time correction was enabled in the OPS for all tests. The complex refractive index of coal (1.78 – *i* 0.60) and density (1220 kg/m^3) were also keyed into the OPS to carry out a conversion of optical particle concentration to gravimetric concentration (Janzen, 1979). Two identical calibrated OPSs were installed upstream and downstream of the Vortecone to report the concentrations.

Airflows of 0.28 m^3/s and 0.38 m^3/s were used for iso-kinetic sampling for investigation of cleaning efficiency. The frequencies on the variable frequency drive (VFD) to precisely establish these flows in the duct were obtained using the flow-pressure drop curve (Fig. 7). Appropriate frequencies were set on the VFD to establish those airflow rates in the ductwork. Cross-sections were traversed upstream and downstream of the Vortecone inside the duct to look for biases in airflow speeds. Points were located where airflow velocity was identical to the average airflow speed in the duct. The tip of the isokinetic sampling probes was pointed into the airflow at those points. This ensured that nominal airflow at those points was not affected due to the presence of the nozzles and aerosol particle distribution at the sampling point was not altered. The tips were interchanged to work with both airflows.

A spray nozzle was used to inject water into the Vortecone at a known flow rate controlled by a digital flowmeter and control valve. Precisely 5.0 gm of coal dust was weighed and injected into the ductwork upstream of the Vortecone at a constant rate over 8.0 min using Arduino controlled auger feeder. This injection rate of coal dust ensured that the OPS was never overwhelmed with a high particle count especially due to a skewed distribution of coal-dust concentration distribution in the feed. This was critical to minimizing the coincidence errors in smaller particles. The tests were repeated three times in random order to eliminate systematic errors in experiments.

4. Results

Iso-kinetic sampling was carried out to determine the size distribution of aerosol particles upstream of the filter and that escape the Vortecone. The log files generated during the experiments were downloaded using the TSI aerosol management software and the particle number concentration converted to mass concentration. Cleaning efficiencies were calculated using the averaged mass concentration values over three tests repeated in a random sequence. Fig. 8 and Fig. 9 show the plots of cleaning efficiency at airflows at 0.28 m^3/s and.38 m^3/s. The plots show that the Vortecone captures a significant number of coal dust particles exceeding 2.0 microns for both the airflows. The cleaning efficiency of the Vortecone improved with the particle size in the airstream. The cleaning efficiency was observed to improve with an increase in airflow

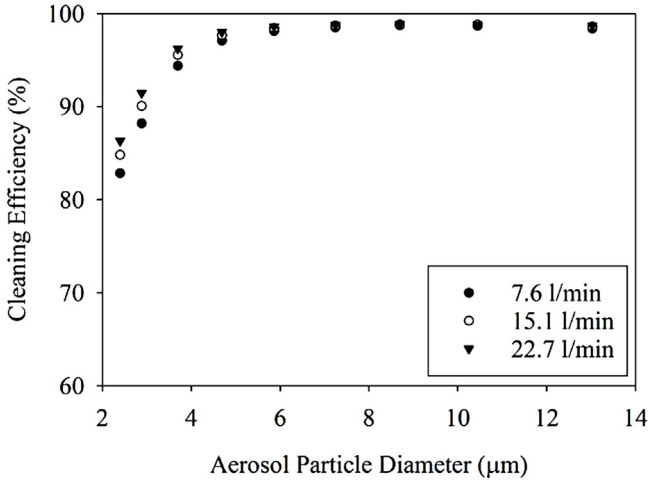

Fig. 9. Cleaning efficiency plot obtained at the airflow of 0.38 m^3/s.

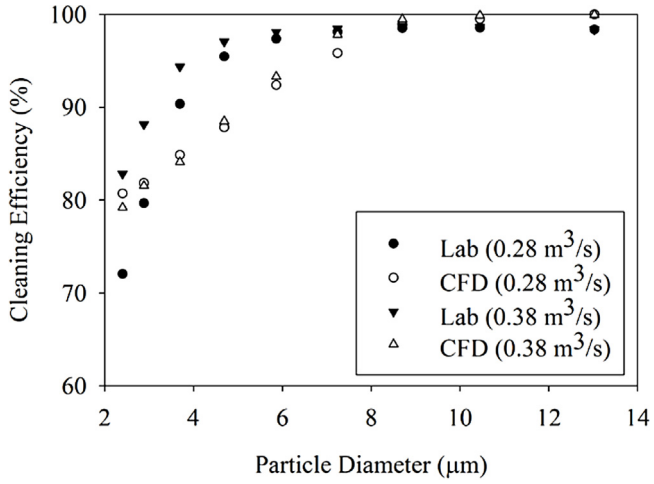

Fig. 10. Sensitivity analysis of the VOF with the cleaning efficiency obtained from lab tests.

since the aerosol particles possess higher momentum now and their trajectory is increasingly difficult to alter. Water flow was not observed to be the contributing factor to the cleaning efficiency. Water serves as a surface cleansing agent and prevents the accumulation of the captured dust particles on the Vortecone surface. Therefore, airflow was found to positively impact the cleaning efficiency whereas water flow was not important once the Vortecone surface was wet.

Both the cleaning efficiency curves were approximated to follow an exponential rise to a maximum trend and could be expressed as shown in Eq.1,

$$\text{Cleaning Efficiency}\,(\%),\ \eta = a\left(1 - e^{-bd}\right) \quad (1)$$

where a and b are constants for a known air and water inflows. The values of a and b were calculated using the SigmaPlot software. The values of corresponding cut-off sizes were also calculated, where d_{75} and d_{90} are the particle diameters having a 75.0 and 90.0% probability of being captured by the Vortecone. The cut-off diameters in all the cases were found to decrease with an increase in airflow through the Vortecone. Particle size with a probability of 75 and 90% capture at 0.28 m^3/s airflow and 15.1 l/min water flow were computed to be 2.6 μm and 4.3 μm respectively. Increasing the water flow to 22.7 l/min had a negligible impact with particle size decreasing to 2.5 μm and 4.2 μm respectively. The particle size decreased to 1.7 μm (1.6 μm at 22.7 l/min) and 2.9 μm (2.7 μm at 22.7 l/min) when the airflow was increased to 0.38 m^3/s. Therefore, no conclusive evidence of the impact of the water flow rate on cleaning efficiency was observed.

A sensitivity analysis of the VOF parameter was carried out to find out the most suitable value to mimic the laboratory test results. Simulations were set up and run using with the VOFs altered in the user-defined script. Numerical cleaning efficiency predicted by the computer models were compared to the laboratory test results. Fig. 10 shows the plots of the predicted cleaning efficiency using the iso-surface of the VOF of 0.001. These plots have been generated for a fixed water inflow of 15.1 l/min. The computer models agreed well with the results obtained from laboratory tests. Differences in computer models and laboratory experiments could be attributed to an unknown distribution of particles at the Vortecone inlet since they were injected pneumatically perpendicular to the duct. The presence of multiple bends with vane and rail arrangements also affects the particle trajectory which could not be captured in computer models.

5. Conclusions

This paper describes the methodology of determining the mechanism of capture in a complicated Vortecone filter with a mixture of CFD and laboratory experiments. Vortecone forces the particle-laden air into rapidly swirling turns which preferentially moves heavier dust towards the periphery. The particles are trapped by water film close to the surface. Large opening dimensions compared to the particles' diameters makes it a non-clogging device. CFD models are critical in the study of this device because it cannot be reliably instrumented without impacting the mechanism of capture. This modeling is complicated by the injection of water into the Vortecone using a spray that is typically found in mining equipment. Simulations were developed to predict the steady-state flow pattern followed by the dynamics of swirling water film. The cleaning efficiency of particles in the Vortecone was realized using a custom user-defined formatted script integrated into the solver.

Laboratory apparatus and experiments were completed to determine the correctness of the CFD models which were developed. Using these techniques, it was shown in both the laboratory experiments and in the CFD modeling that airflow is the most important factor regarding the capture inside the filter. Water flow is important to clear the captured dust out of the filter but does not have a large influence on the overall capture efficiency.

These results show that the airflow is the design constraint and for any use of the Vortecone. Coal-dust particle cleaning efficiency was found to exceed 75% for particles 2.8 μm in size and 90% for 4.7 μm for all airflows. The CFD model should be used to calculate the size of the physical Vortecone. Water should be introduced into the application, but it is not necessary to flood the filter. Further work should be done investigating reuse of the water used in the filter.

Declaration of Competing Interest

The authors do not have any conflict of interests.

Acknowledgment

The authors express their gratitude to the National Institute for Occupational Safety and Health for funding the research project. The project is aimed at alleviation of dust in underground coal mines. The authors also acknowledge Dr. Thomas Novak of the Department of Mining Engineering and Dr. Kozo Saito of the Department of Mechanical Engineering, the University of Kentucky for his invaluable suggestions. The authors acknowledge Dr. Emily Sarver

of the Department of Mining and Minerals Engineering at Virginia Tech for assistance with optical particle counting sensor.

References

Petavratzi, E., Kingman, S., Lowndes, I., 2005. Particulates from mining operations: a review of sources, effects and regulations. Miner. Eng. 18, 1183–1199.

Arnold, C., 2016. A scourge returns: black lung in Appalachia. Environ. Health Perspect. 124 (1), A13–A18.

Laney, A., Weissman, D., 2014. Respiratory disease caused by coal mine dust. Journal of Occupational Medicine 10, 18–22.

Zheng, Y., Feng, C., Jing, G., Qian, X., Li, X., Liu, Z., Huang, P., 2009. A statistical analysis of coal mine accidents caused by coal dust explosions in China. J. Loss Prev. Process Ind. 22 (4), 528–532.

MSHA, 2014a. Data and Reports: Upper Big Branch Mine-South, Performance Coal Company. United States Department of Labor.

MSHA, 2002. Report of Investigation : Fatal Underground Coal Mine Explosions, September 23, 2001, Jim walter Resources. United States Department of Labor, Arlington, VA.

MSHA, 1969. Federal Mine Health and Safety Act of 1969 (Mine Act, Public Law 91-173). United States Department of Labor.

MSHA, 1977. Federal Mine Safety and Health Act of 1977 (Mine Act, Public Law 95-164). United States Department of Labor.

MSHA, 2014b. Federal Register Vol. 79, No. 84. Lowering Miners' Exposure to Respirable Coal Mine Dust, Including Continuous Personal Dust Monitors; Final Rule. United States Department of Labor.

Pollock, D., Organiscak, J., 2007. Airborne dust capture and induced airflow of various spray nozzle designs. Aerosol Sci. Technol. 41 (7), 711–720.

Calvert, S., 1974. Engineering design of fine particle scrubbers. J. Air Pollut. Control Assoc. 24 (10), 929–934.

Eckert, J., Stringle, J.R.F., 1974. Performance of wet Scrubbers on liquid and solid particulate matter. J. Air Pollut. Control Assoc. 24 (10), 961–966.

Campbell, A., Moynihan, D., Roper, W., Willis, E., 1983. Dust Control System and Method of Operation.

Colinet, J., Reed, W., Potts, J., 2013. Dust Levels When Operating a Flooded-bed Dust Scrubber Scrubber in 20 - Foot Cuts. Pittsburgh, PA.

Wedding, W., Novak, T., Arya, S., Kumar, A., 2015. CFD modeling of a flooded-bed dust scrubber concept for longwall shearer operating in a US coal seam. In: 15th North American Mine Ventilation Symposium, Blacksburg, VA.

Thomas, D., Penicot, P., Contal, P., Vendel, J., 2001. Clogging of fibrous filter by solid aerosol particles - Experimental and modeling study. Chem. Eng. Sci. 56 (11), 3549–3561.

Calle, S., Bemer, D., Thomas, D., Contal, P., Leclerc, D., 2001. Changes in the performances of filter media during clogging and cleaning cycles. Ann. Occup. Hyg. 45 (2), 115–121.

Agranovski, I., Shapiro, M., 2001. Clogging of wet filters by dust particles. J. Aerosol Sci. 32, 1009–1020.

Kanaoka, C., Hiragi, S., 1990. Pressure drop of air filter with dust load. J. Aerosol Sci. 21 (1), 127–131.

Marple, V., Willeke, K., 1967. Impactor design. Atmos. Environ. 10 (10), 891–896.

Newton, G., Raabe, O., Mokler, B., 1977. Cascade impactor design and performance. J. Aerosol Sci. 8 (5), 339–347.

A. J. Salazar, K. Saito, R. P. Alloo and N. Tanaka, Wet scrubber and paint spray booth including the wet scrubber. European Patent Application. Patent EP 1 258 294 A2, 23 August 2002.

A. J. Salazar, K. Saito, R. P. Alloo and N. Tanaka, Wet scrubber and paint spray booth including the wet scrubber. United States Patent 6,093,250, 25 July 2000.

Krames, J., Buttner, H., 1994. The cyclone scrubber - a high efficiency wet separator. Chem. Eng. Technol. 17 (2), 73–80.

Dahneke, B., 1971. The capture of aerosol particles by surfaces. J. Colloid Interface Sci. 37 (2), 342–353.

Celik, I.B., Ghia, U., Roache, P., Freitas, C.J., Coleman, H., Raad, P.E., 2008. Procedure of estimation and reporting of uncertainty due to discretization in CFD applications. J. Fluids Eng. 22.

Hirt, C., Nicholas, B., 1981. Volume of fraction (VOF) method for the dynamics of free boundaries. J. Comput. Phys. 39, 201–225.

Cunningham, E., 1910. On the velocity of steady fall of spherical particles through fluid medium. Proc. Royal Soc. (Lond) A 33, 357–365.

Tsai, C., Pui, D., Liu, B., 1990. Capture and rebound of small particles upon impact with solid surfaces. Aerosol Sci. Technol. 12 (3), 497–507.

Wilcox, J., 1956. Isokinetic flow and sampling. J. Air Pollut. Control Assoc. 5 (4), 226–245.

Janzen, J., 1979. The refractive index of colloidal carbon. J. Colloid Interface Sci. 69 (3), 436–447.